Novel biomaterial-based synovial fluid analysis reveals protective microRNA signatures in a mouse model of acute synovitis-driven osteoarthritis

Authors

Kei Takahata1, Kohei Arakawa2, Takashi Yasuda3, Saaya Enomoto4, Takuya Katashima5, Sakai Takamasa5, Takanori Kokubun1, 6*

Affiliations

1 Graduate School of Health, Medicine, and Welfare, Saitama Prefectural University, Saitama, Japan

2 Laboratory of Animal Regeneration Systemology, Department of Life Sciences, School of Agriculture, Meiji University, Kanagawa, Japan

3 Faculty of Advanced Life Sciences, Hokkaido University, Hokkaido, Japan

4 Saitama Prefecture General Rehabilitation Center, Saitama, Japan

5 Graduate School of Engineering, The University of Tokyo

6 Department of Physical Therapy, School of Health and Social Services, Saitama Prefectural University, Koshigaya, Saitama, Japan

Correspondence

[1, 6]Takanori Kokubun, Ph.D.

820 San-nomiya, Koshigaya, Saitama, 343-8540. Japan

Tel: +81 48-973-417617

kokubun-takanori@spu.ac.jp

Abstract

Objective: Synovial fluid micro-RNAs have been investigated to clarify the Osteoarthritis (OA) development, however, analyzing them in the murine models had not been established. The purpose of this study was to develop a novel biomaterial-based method to collect murine synovial fluid and elucidate onset mechanism of OA with acute synovitis and chronic mechanical stress.

Method: Twelve-week-old C57BL/6J males (n = 72) were divided to the ACL-Transection (ACL-T), ACL-rupture (ACL-R), and Intact groups. We performed joint instability test and histological analysis for cartilage degeneration and synovitis at 2, 6, and 10 weeks. Real time PCR was conducted for articular cartilage at 2 weeks and synovium at 2, 6, and 10 weeks. Tetra-slime was injected into the knee joint and solidified slime including synovial fluid was analyzed in digital PCR at 2 weeks.

Results: No difference was observed in joint instability between both ACL injury models. Unlike the Control and ACL-R groups, acute synovitis and secondary cartilage degeneration were induced in the ACL-T group at 2 weeks. The ACL-T group also exhibited an increase of Mmp-3, Tnf-α, Ifn-γ, and inos in synovium, and miR145-5p and miR149-5p in synovial fluid compared to the ACL-R group. However, no histological and biological differences were observed at 6 and 10 weeks.

Conclusion: We successfully analyzing synovial fluid miRNAs in mice model using Tetra-Slime. Acute synovitis caused secondary cartilage degeneration through MMP-3, TNF-α, and M1 macrophage activation in synovium during the early stage, whereas miR145-5p and miR149-5p in synovial fluid were upregulated to prevent the progression. However, mechanical stress had a much greater impact on cartilage degeneration in the long run rather than synovitis.

Key Words:

Osteoarthritis, Synovial fluid, Synovitis, Mechanical stress, miRNA, biomaterials

86 # Introduction

87 Knee Osteoarthritis (OA) is one of the most common musculoskeletal diseases,
88 characterized by whole−joint pathology, including synovitis and subchondral bone sclerosis,
89 resulting from cartilage degeneration[1]. These structural changes affect each other via synovial
90 fluid and progress irreversibly, as articular cartilage is avascular and has a poor healing
91 capacity. To achieve the prevention of cartilage degeneration, elucidating the intra-articular
92 changes that occur during early OA progression before cartilage degeneration is required;
93 however, it is assumed that early detection is difficult in humans due to the variability of
94 symptoms and disease progression in the early stages of cartilage degeneration. [2, 3]

95 In the knee joint space, synovial fluid fills and mediates bidirectional interaction
96 between the joint tissues. Synovial fluid is an ultrafiltrate of blood plasma and is primarily
97 composed of hyaluronan and lubricin, which play a significant role as a joint space lubricant
98 and a nutrient source for intra-articular tissues. [4] Previous studies have reported that
99 Interleukin (IL)-6, IL-8, and Tumor Necrosis Factor (TNF)-α in synovial fluid are correlated
100 with OA severity [5]. Additionally, Matrix Metalloproteinase (MMP)-3 could be a biomarker
101 for detecting early-stage OA. [6] Furthermore, circulating microRNAs (miRNAs) in the
102 synovial fluid have been recently highlighted as a novel biomarker. [7] miRNAs are short, non-
103 coding RNAs that are typically 18-25 nucleotides in length, which are used to investigate
104 various diseases as they are stable compared to other RNAs degraded by ribonucleases.[8] It has

105 been reported that miR-23a-3p, miR-24-3p, miR-27b-3p, miR-29c-3p, miR-34a-5p, and miR-
106 186-5p in the synovial fluid were expressed in the late-stage OA compared to the early-stage.
107 [9] In addition, synovial fluid miR-210 increased significantly in the early and late-stage OA
108 than in healthy individuals. [10] Therefore, synovial fluid has been identified as a potential
109 target to detect the intra-articular environment in the OA progression. Many clinical studies
110 have been investigating the synovial fluid biomarker to find OA earlier in human [11], which
111 has yet to be established. Thus, preclinical experiments using animal models are crucial for
112 understanding the mechanism of OA onset. However, synovial fluid analysis, especially for
113 miRNAs in rodent models, is limited because the amount of synovial fluid is tiny. In a few
114 studies, joint lavage was performed as follows: 25-50 μL of saline was initially injected into
115 the knee joint, and then the synovial fluid was drawn out.[12-14] However, it is difficult to
116 collect a sufficient amount of synovial fluid and present relevant data due to the tiny knee
117 joints in mice.[15]
118 Recently, many kinds of biomaterials were developed and applied for drug-
119 deliveries, tissue engineering, and medical diagnostics. [16-18] Tetra-slime is composed of
120 reversible boronic ester bonds between phenylboronic acid and diol groups, and its hardness
121 can be changed by adjusting the precursor concentration and pH. Moreover, it can also be
122 dissolved by sorbitol as sugars attach to phenylboronic acid and cleave ester bonds. [19] Based
123 on these material properties, we hypothesized that harvesting and dissolving the solidified

124 Tetra-Slime, which was injected into the knee joint, would allow for the efficient collection of
125 synovial fluid. The purpose of this study was to develop a novel method to analyze synovial
126 fluid miRNAs in murine knee joints using biomaterials, Tetra-slime,[20] instead of joint lavage
127 methods to reveal the onset mechanism of knee OA based on the synovial fluid dynamics.
128 Using this method in surgical Anterior Cruciate Ligament Transection (ACL-T) and Non-
129 Invasive ACL rupture (ACL-R) mice models, we aimed to elucidate the characteristics of
130 each rodent model in terms of inflammation and serve fundamental insights to understand
131 human pathology in detail.
132

133 # MATERIALS AND METHODS

134 **Animals and Experimental Design**

135 This study was approved by the Animal Research Committee of Saitama Prefectural
136 University (approval number: 2020-6). The animals were handled according to relevant
137 legislation and institutional guidelines for humane animal treatment. Seventy-two 12-week-
138 old C57BL/6 male mice were randomized into the Invasive ACL-T group (n = 36) and Non-
139 Invasive ACL-R group (n = 36). The contralateral knee joint in the ACL-R group was used as
140 the control group. Six mice in each group were sacrificed at 2, 6, and 10 weeks, and the target
141 tissues were collected for each analysis (Fig. 1). All mice were housed in plastic cages under a

12-hour light/dark cycle. The mice were allowed unrestricted movement within the cage and had free access to food and water.

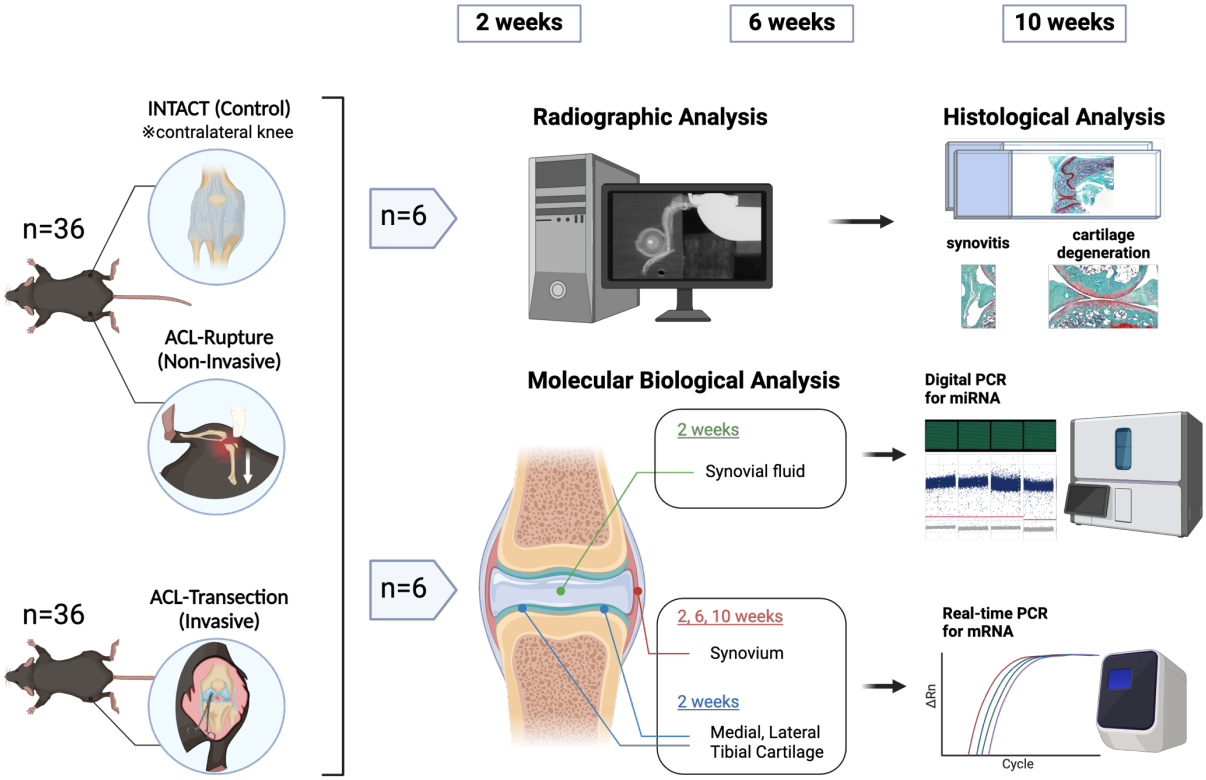

Fig. 1. Experimental design. We made the Invasive ACL-T, Non-Invasive ACL-R, and Control groups. Contralateral knee in the ACL-R model was used as Control group. At 2, 6, and 10 weeks, anterior drawer test and histological analysis for synovitis and cartilage denegation in the medial and lateral compartments were performed. Articular cartilage at 2 weeks and synovium at 2, 6, and 10 weeks were harvested, and mRNAs were analyzed in real time PCR. In addition, synovial fluid was collected at 2 weeks and miRNAs level were assessed.

Creating ACL-T and ACL-R models

All procedures were performed on the left knee joint of each mouse under a combination of anesthetics (medetomidine, 0.375 mg/kg; midazolam, 2.0 mg/kg; and

157 butorphanol, 2.5 mg/kg). The medial joint capsule was cut to expose the intra-articular joint.
158 ACL was transected with scissors to avoid causing injuries to other tissues. After checking the
159 anterior tibial translation manually, the joint capsule and skin incision were closed with 5-0
160 nylon threads. The ACL-R model was created based on our previous study.[21] Briefly, the knee
161 joint was fixed at 90 degrees using surgical tape on a stand, then the force along the long axis
162 of the femur was applied by the thumb's tip slowly and carefully. Applied force was stopped
163 quickly after hearing a distinct popping sound, which indicates ACL rupture; thereafter,
164 anterior tibial translation was confirmed manually as well.
165
166 **Ex vivo radiographic analysis for knee joint instability**
167 After dissection at each time point, knee joints were collected (each group, n = 6) and
168 an anterior drawer test was performed to evaluate joint instability (Fig. 2A). Based on our
169 previous study [21, 22], the proximal tibia was pulled forward with a constant force spring (0.05
170 kgf; Sanko Spring Co., Ltd., Fukuoka, JPN), and X-ray images were taken at this position. In
171 the acquired image, the tibial tuberosity and the anterior end of the femoral condyle were set
172 as landmarks, then the anterior tibial displacement was measured by the linear distance from
173 the perpendicular line from the anterior end of the femoral condyle to the tibial tuberosity
174 using Image J (National Institutes of Health, Bethesda, MD, USA).
175

176 **Histological analysis for cartilage degeneration and synovitis**

177 Knee joints were fixed using 4% paraformaldehyde for 1 day, decalcified in 10%
178 ethylenediaminetetraacetic acid for 2 weeks, dehydrated in 70% and 100% ethanol and
179 xylene, and embedded in paraffin blocks after performing radiographic analysis. The samples
180 were cut in the sagittal plane (thickness, 7 μm) using a microtome (ROM-360; Yamato Kohki
181 Industrial Co., Ltd., Saitama, JPN). Then, safranin-O/fast green staining was performed to
182 assess the articular cartilage degeneration with the Osteoarthritis Research Society
183 International (OARSI) histopathological grading system [23] and synovitis score [24] in the medial
184 and lateral compartments. These scores were assessed by two independent observers blinded
185 to all other sample information. We evaluated the contact area not covered by the meniscus on
186 the tibial plateau and the synovium located inside the infrapatellar pad. The mean of the
187 observer's scores was used as a representative value.

188

189 **Real-time PCR for articular cartilage and synovium**

190 Articular cartilage on the medial and lateral tibial plateau at 2 weeks and synovium at
191 2, 6, and 10 weeks were collected and stored in a deep freezer until analysis (each group, n =
192 6). Based on the manufacturer’s instructions, total RNA was extracted from these tissues
193 using the ISOGEN (NIPPON GENE CO., LTD., Tokyo, JPN). cDNA synthesis was
194 performed from the total RNA by Thermal Cycler Palm-Cycler (Corbett Research, SYD,

195 AUS) with High-Capacity cDNA Reverse Transcription kit (Applied Biosystems, CA, USA).

196 Subsequently, real-time PCR was conducted to assess the expression of following genes using

197 the StepOne-Plus system (Applied Biosystems, Waltham, MA, USA); *Mmp-*

198 *3*(Mm00440295), Tissue inhibitor of metalloproteinase-1 (*Timp-1:* Mm01341361),

199 Transforming growth factor-β1 (*Tgf-β1:* Mm01178820), *Tnf-α* (Mm00443258), *Il-1β*

200 *(*Mm00434228), *Il-6* (Mm00446190), *Il-10* (Mm01288386), Interferon-γ (*Ifn-*

201 *γ* :Mm01168134), inducible nitric oxide synthase（*inos* :Mm00440502_m1), and Toll like

202 receptor-4 (*Tlr4* :Mm00445273_m1). We used Glyceraldehyde-3-phosphate dehydrogenase

203 (*Gapdh* :Mm99999915) as a housekeeping gene, and relative expression of genes was

204 detected by the 2-△△Ct method [25].

205

206 **Digital PCR for synovial fluid miRNA using Tetra-Slime**

207 In this study, we selected the Tetra-slime to collect the murine synovial fluid. 4-arm

208 PEG BFA and 4-arm PEG Gluconic (XIAMEN SINOPEG BIOTECH CO., LTD., Fujian,

209 CHN) were resolved with 50 mM phosphate-buffered saline (pH 3.0) to adjust 0.2 g/ml

210 concentration respectively. We injected both solutions by 25 μL into the knee joint for live

211 mice, then kept the needle for a while to avoid leaking the solution (Fig. 7A). After 3 minutes,

212 mice were sacrificed and the quadriceps and patellar were removed to expose the intra-

213 articular joints, then solidified Tetra-Slime was collected. We added 100 μL of sorbitol

214 solution with a 0.5 g/ml concentration to the collected Tetra-Slime and stirred slowly to
215 dissolve and separate from the surrounding intra-articular tissue, then obtained the pure
216 solution with synovial fluid biomolecules released. Based on the manufacturer's instructions,
217 miRNA was extracted from the synovial fluid solution using the miRNeasy Micro Kit
218 (QIAGEN, LTD. Tokyo, JPN). cDNA synthesis was performed by QIAamplifier 96
219 (QIAGEN, LTD. Tokyo, JPN) with miRCURY LNA RT Kit (QIAGEN, LTD. Tokyo, JPN).
220 Subsequently, digital PCR (dPCR) was conducted using the QIAcuity One (QIAGEN, LTD.
221 Tokyo, JPN) and target genes were *hsa-miR-145-5p* (YP00204483) and *hsa-miR-149-5p*
222 (YP00204321). We normalized the target gene with the housekeeping gene, 5S rRNA
223 (YP00203906), for each sample, and then calculated the relative expression level by
224 standardizing with the Control group. UniSp6 (YP00203954) was also used as a spike-in
225 control.
226

227 **Statistical analysis**

228 Statistical analysis was performed using RStudio version 1.4.1106. For the results of
229 anterior tibial displacement by the anterior drawer test, relative expression of genes in
230 synovium and cartilage by real-time PCR, and miRNA data measured using dPCR, one-way
231 analysis was performed initially, then the Tukey-Kramer test was used as a post-hoc test. We
232 utilized the value of ΔCt for the real-time PCR data and the relative expression value for the

dPCR data. Whereas the Kruskal-Wallis test was used to compare the OARSI and synovitis scores, and the Steel-Dwass method was used for the subsequent multiple comparisons. Parametric data are expressed as the means ± 95% confidence intervals (CI); in contrast, the non-parametric data are expressed as the medians ± interquartile ranges. Statistical significance was set at $p < 0.05$. CIs were shown in the Supplementary data.

Results

ACL-T and ACL-R groups showed similar joint instability

The anterior displacement in the ACL-T and ACL-R groups was significantly higher than that in the Control groups at 2 weeks (ACL-T vs. Control, $p < 0.001$, ACL-R vs. Control, $p < 0.001$), 6 weeks (ACL-T vs. Control, $p < 0.001$, ACL-R vs. Control, $p < 0.001$), and 10 weeks (ACL-T vs. Control, $p < 0.001$, ACL-R vs. Control, $p < 0.001$). However, there was no significant difference between the ACL-T and ACL-R groups at all time points. These results suggested that the effect of mechanical stress on OA progression was identical in both ACL-deficient models.

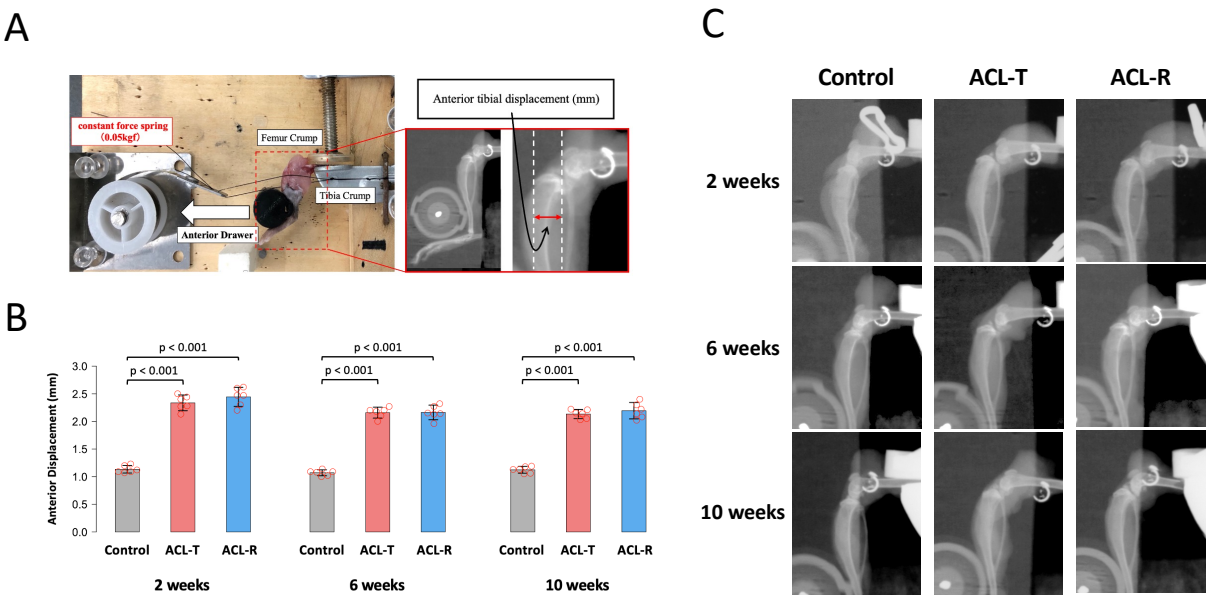

Fig. 2. Evaluation of the joint instability *ex vivo* using soft X-ray and original anterior drawer device. At 2, 6, and 10 weeks, the amount of anterior tibial displacement was significantly increased in the ACL-T and ACL-R groups compared to that in the Control group. However, there was no significant difference between both ACL injury models. Data are presented as the mean ± 95% CI.

ACL-T group induced acute synovitis in the early stage

For the medial compartment, severe synovitis with increased cellularity, enlargement of the synovial lining cell layer, and inflammatory infiltration was observed in the ACL-T group (Fig. 3A). Moderate synovitis with cell multiplication and cell layer enlargement was confirmed in the ACL-R group. Compared with the Control group, synovitis score was significantly higher in the ACL-T group ($p = 0.009$) and ACL-R group ($p = 0.012$) (Fig 3B). Interestingly, ACL-T group increased score significantly compared with the ACL-R group ($p = 0.032$). At 6 weeks, moderate synovitis characterized by some enlargement and increased cellularity developed in both ACL-deficient groups, and the synovitis score in the ACL-T

264 group ($p = 0.01$) and ACL-R group ($p = 0.01$) was significantly higher than in the Control

265 group. At 10 weeks, similar moderate to severe synovitis was observed in both ACL-deficient

266 groups, and the synovitis score in the ACL-T group ($p = 0.009$) and ACL-R group ($p = 0.01$)

267 was significantly elevated compared to the Control group.

268 For the lateral compartment, moderate and mild synovitis occurred in both ACL-

269 deficient groups. Synovitis score was significantly higher in the ACL-T group ($p = 0.009$) and

270 ACL-R group ($p = 0.01$) compared with the Control group (Fig. 3C-D). At 6 and 10 weeks,

271 moderate synovitis was observed in the ACL-T and ACL-R groups, and both synovitis scores

272 increased significantly compared with the Control group (6 weeks: ACL-T vs. Control, $p =$

273 0.01; ACL-R vs. Control, $p = 0.013$, 10 weeks: ACL-T vs. Control, $p = 0.016$; ACL-R vs.

274 Control, $p = 0.01$).

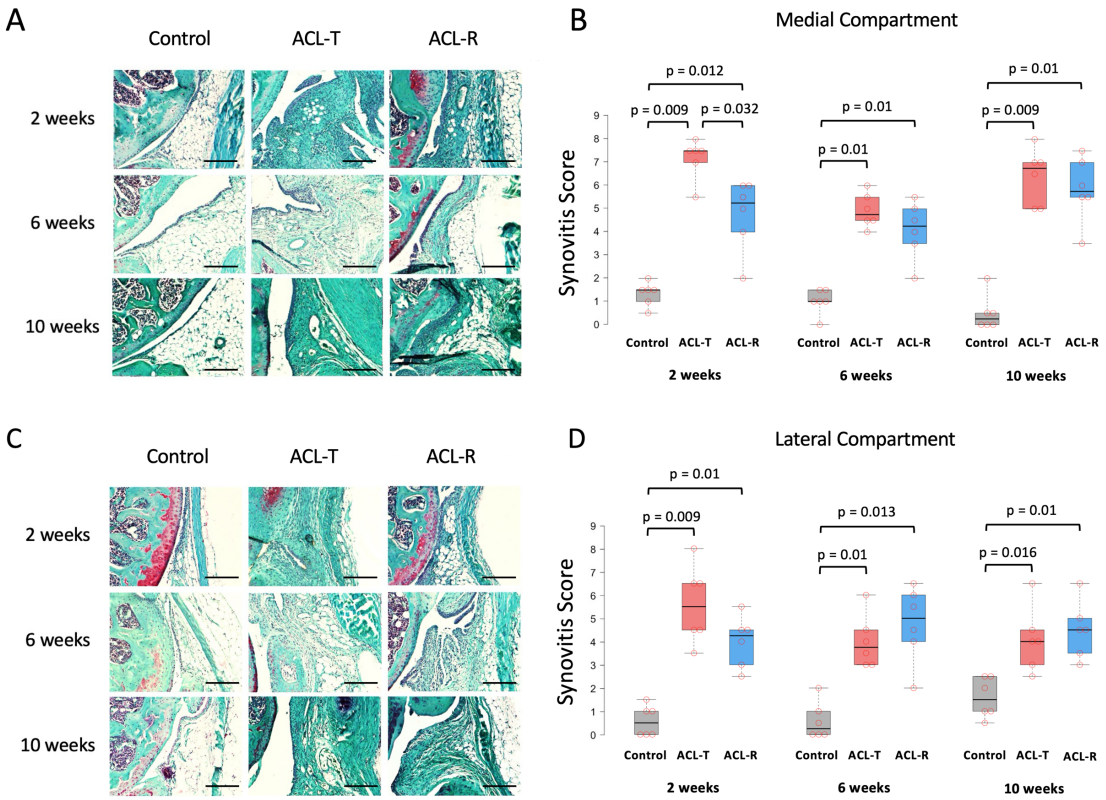

Fig. 3. Histological analysis of synovitis using safranin-O/fast green staining and synovitis score. (A-B) In the medial compartment, the synovitis score in the ACL-T and ACL-R groups was significantly higher than that in the Control group at 2 weeks. Moreover, the score in the ACL-T group was also elevated significantly compared to the ACL-R group. At 6 and 10 weeks, both ACL injury groups significantly increased the synovitis score compared with the Control group. (C-D) In the lateral compartment, the ACL-T and ACL-R groups exhibited a significant increase of synovitis score compared to the Control group at all timepoints. Data are presented as the median ± interquartile range. Black scale bar, 100 μm.

Secondary cartilage degeneration was induced by acute synovitis in the ACL-T group

To examine the tissue interaction between early synovitis and cartilage degeneration, histological analysis was performed. For the medial compartment, some fibrillation of the superficial cartilage was observed in the ACL-T and ACL-R groups at 2 weeks (Fig. 4A). Additionally, small clefts and loss of cartilage were confirmed only in the ACL-T group. The

290 OARSI score of the ACL-T group was significantly higher than that of the Control group (p =
291 0.009) (Fig. 4B). At 6 weeks, cartilage fibrillation and mild to moderate vertical cracks into
292 the calcified layer developed in both ACL-deficient groups. Compared with the Control
293 group, the OARSI score was significantly elevated in the ACL-T group (p = 0.022) and ACL-
294 R group (p = 0.014). At 10 weeks, moderate to severe cartilage degeneration with loss of the
295 superficial layer was observed in both ACL-deficient groups. Compared with the Control
296 group, the OARSI score significantly increased in the ACL-T group (p = 0.01) and ACL-R
297 group (p = 0.01).

298 For the lateral compartment, cartilage degeneration with loss of safranin staining,
299 small fibrillation, and vertical clefts was confirmed in the only ACL-T group at 2 weeks (Fig.
300 4C). The OARSI score in the ACL-T group was significantly higher compared with that in
301 the Control group (p = 0.018) and ACL-R group (p = 0.02) (Fig. 4D). At 6 weeks, small
302 fibrillation and clefts in the superficial cartilage layer occurred in both ACL-deficient groups;
303 however, there was no significant difference in the OARSI score between all groups. At 10
304 weeks, mild cartilage degeneration with small fibrillation and vertical clefts in the superficial
305 cartilage layer was observed in both ACL-deficient groups. Compared with the Control
306 group, the OARSI score was significantly higher in the ACL-T group (p = 0.012) and ACL-R
307 group (p = 0.044). In summary of the histological analysis, the ACL-T group induced acute
308 synovitis and cartilage degeneration in the first 2 weeks compared with the ACL-R group,

309 although no difference in the joint instability. Cartilage degeneration in both ACL-deficient

310 models progressed in the late stage, as well as synovitis.

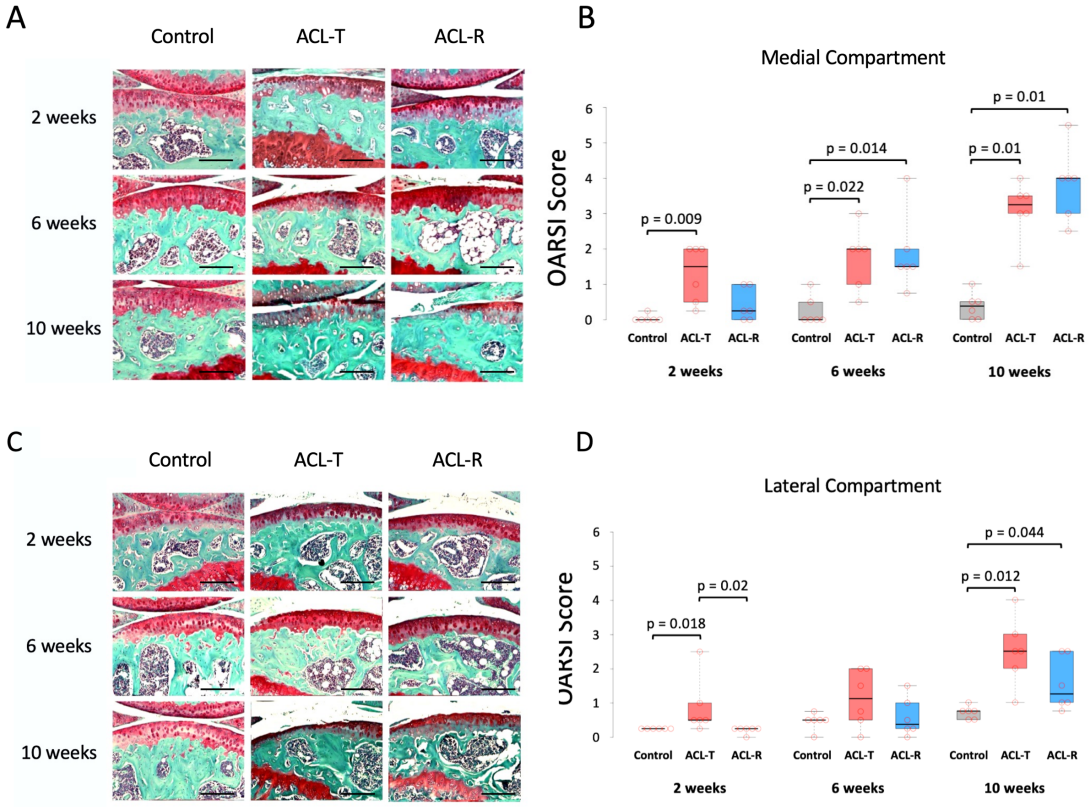

311

312 Fig. 4. Histological analysis of cartilage degeneration using safranin-O/fast green staining and
313 OARSI score. (A-B) In the medial compartment, the OARSI score in the ACL-T group was
314 significantly higher than that in the Control group at 2 weeks. At 6 and 10 weeks, both ACL
315 injury groups significantly increased the OARSI score compared with the Control group. (C-
316 D) In the lateral compartment, the OARSI score in the ACL-T group increased significantly
317 compared the Control and ACL-R groups at 2 weeks. At 10 weeks, both ACL injury groups
318 exhibited a significant increase of OARSI score compared to the Control group. Data are
319 presented as the median ± interquartile range. Black scale bar, 100 μm.

320

321

322

323 **ACL-R group induced catabolic factors and inflammation cytokine expression in the**

324 **articular cartilage**

325 To explore the molecular mechanism between acute synovitis and cartilage

326 degeneration, we performed real-time PCR for the articular cartilage at 2 weeks because

327 cartilage degeneration occurred in the whole area moderately after 6 weeks. In the medial

328 tibial cartilage compared with the Control group, ACL-T group significantly increased the

329 expression of *Mmp-3* ($p < 0.001$), *Timp-1* ($p = 0.009$), and *Tnf-α* ($p = 0.008$) (Fig. 5A-C).

330 ACL-R group also significantly exhibited an increase of *Mmp-3* ($p < 0.001$), *Timp-1* ($p <$

331 0.001), and *Tnf-α* ($p < 0.001$) compared with the Control group. Moreover, *Tnf-α* in the ACL-

332 R group was significantly higher than in the ACL-T group ($p = 0.005$) (Fig. 5C).

333 In the lateral tibial cartilage, ACL-T group significantly exhibited an increase of

334 *Mmp-3* ($p < 0.001$) and *Timp-1* ($p = 0.036$) compared with the Control group (Fig. 5E-F).

335 *Mmp-3*, *Timp-1*, and *Tnf-α* in the ACL-R group were significantly upregulated compared with

336 the Control group (*Mmp-3*; $p < 0.001$, *Timp-1*; $p < 0.001$, *Tnf-α*; $p = 0.008$) and ACL-T group

337 (*Mmp-3*; $p = 0.03$, *Timp-1*; $p = 0.036$, *Tnf-α*; $p < 0.001$) (Fig. 5E-G). However, no significant

338 differences were observed in the *Ifn-γ* between all groups for the medial and lateral tibial

339 cartilage (Fig. 5D, H). *Tgf-β1*, *Il-1β*, *Il-6*, and *Il-10* were exhibited in the Supplementary

340 Figure 1.

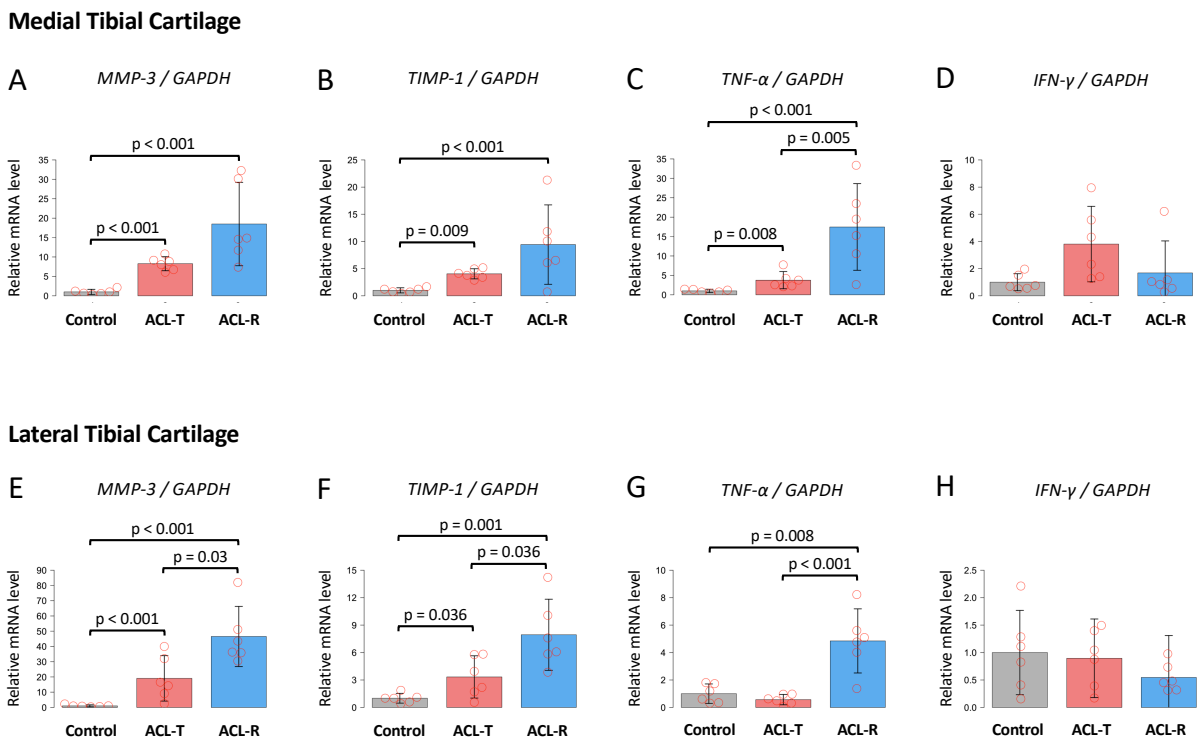

Fig. 5. Real time PCR analysis for medial and lateral tibial articular cartilage at 2 weeks. (A-D) In the medial cartilage, *Mmp-3*, *Timp-1*, and *Tnf-α* expression in the ACL-T and ACL-R groups were significantly increased compared to that in the Control group. In addition, the ACL-R group exhibited a significant increase of *TNF-α* compared to the ACL-T group. (E-H) In the lateral cartilage, the expression of *Mmp-3*, *Timp-1*, and *Tnf-α* in both ACL injury groups were significantly upregulated compared to that in the Control group. *Mmp-3* and *Timp-1* were also significantly increased in the ACL-R group compared to the ACL-T group. Data are presented as the mean ± 95% CI.

ACL-T group increased the expression of catabolic factors, inflammatory cytokines, and M1 macrophage markers in the synovium

At 2 weeks, *Mmp-3* expression was significantly higher in the ACL-T group ($p < 0.001$) and ACL-R group ($p < 0.001$) than the Control group (Fig. 6A). Furthermore, the ACL-T group also exhibited an increase of *Mmp-3* expression significantly compared with the ACL-R group ($p = 0.048$). *Timp-1* was elevated significantly in the ACL-T ($p = 0.002$)

357 and ACL-R group ($p < 0.001$) compared with the Control group (Fig. 6B). The ACL-T group

358 significantly increased *Tnf-α*, *Ifn-γ*, and *inos* compared with the Control (*Tnf-α*; $p = 0.001$, *Ifn-*

359 *γ*; $p = 0.021$, *inos*; $p = 0.017$) and ACL-R group (*Tnf-α*; $p = 0.004$, *Ifn-γ*; $p = 0.012$, *inos*; $p =$

360 0.009) (Fig. 6C-E). However, no significant difference was observed in the *Tlr4* expression

361 among groups (Fig. 6F). The results for *Tgf-β1*, *Il-1β*, *Il-6,* and *Il-10* at 2 weeks, all results at

362 6 weeks, and 10 weeks were described in the Supplementary Figures 2-4.

363 In summary, the RT-qPCR results showed the increased expression of the *Mmp-3*,

364 *Timp-1* of *Mmp-3* inhibitor [26], and *Tnf-α* in cartilage of the ACL-R group, although it induced

365 less synovitis and cartilage degeneration. Unlike the results of cartilage, synovium in the

366 ACL-T group showed upregulation of *Ifn-γ,* M1 macrophage polarization factor, and *iNos*,

367 M1 macrophage marker[27-30] , in addition to *Mmp-3* and *Tnf-α*. However, the *Mmp-3* and *Tnf-α*

368 expressions were not increased at 6 and 10 weeks.

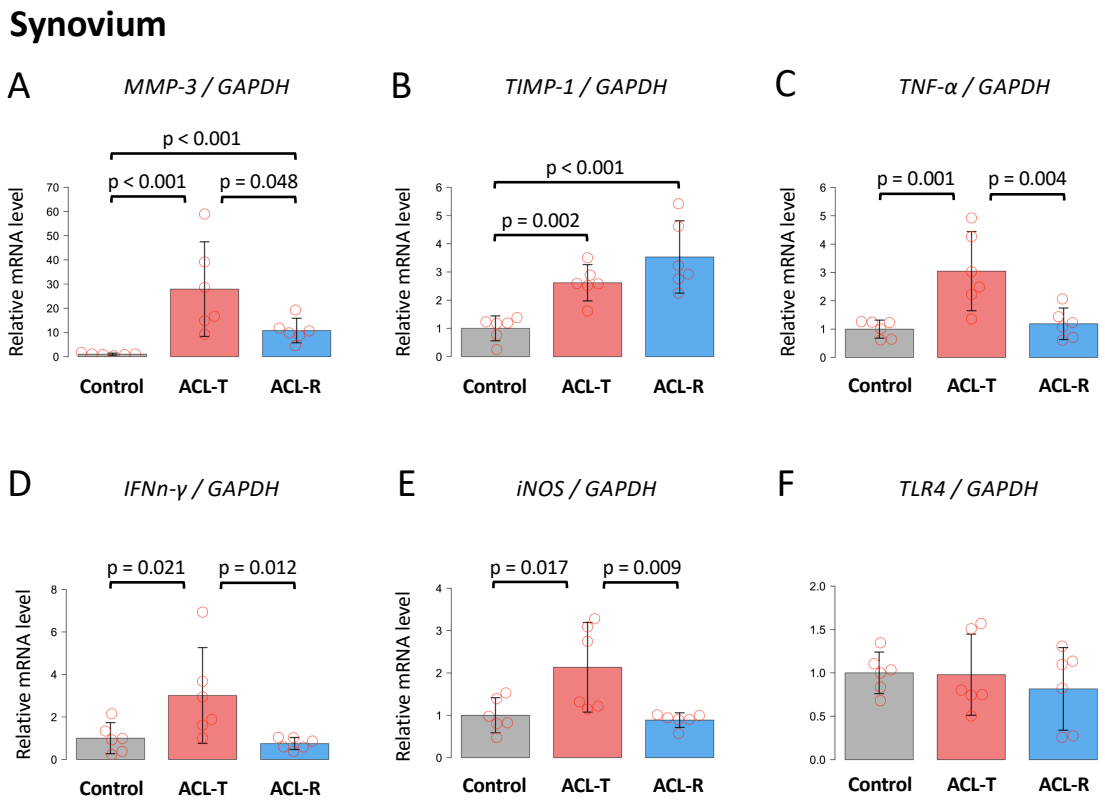

Fig. 6. (A) Real time PCR analysis for synovium at 2 weeks. (A) *Mmp-3* expression in the ACL-T and ACL-R groups were significantly higher than that in the Control group. Moreover, the ACL-T group also significantly increased it compared to the ACL-T group. (B) *Timp-1* in both ACL injury groups was upregulated compared to that in the Control group. (C-E) The ACL-T group exhibited a significant increase of *Tnf-α, Ifn-γ, and inos* compared to the Control and ACL-R group. (F) No difference was observed in the *Tlr4* expression level between groups. Data are presented as the mean ± 95% CI.

The expression of miR145-5p and miR149-5p in the synovial fluid increased in the ACL-T group

To verify the effect of using biomaterial for dPCR, we initially analyzed 5S rRNA expression in only Tetra-Slime as a negative control. Compared with the Tetra-slime including synovial fluid, concentration of 5s rRNA in only Tetra-Slime group was obviously lower although Unisp6 of spike-in control was observed (Supplementary Figure 5). The

expression of miR145-5p[31] and miR149-5p[32, 33], which are downregulated by TNF-α, was investigated. dPCR results showed the increased expression of *miR145-5p* and *miR149-5p* in the ACL-T group compared with other groups, although this difference was not statistically significant (Fig. 7B, C).

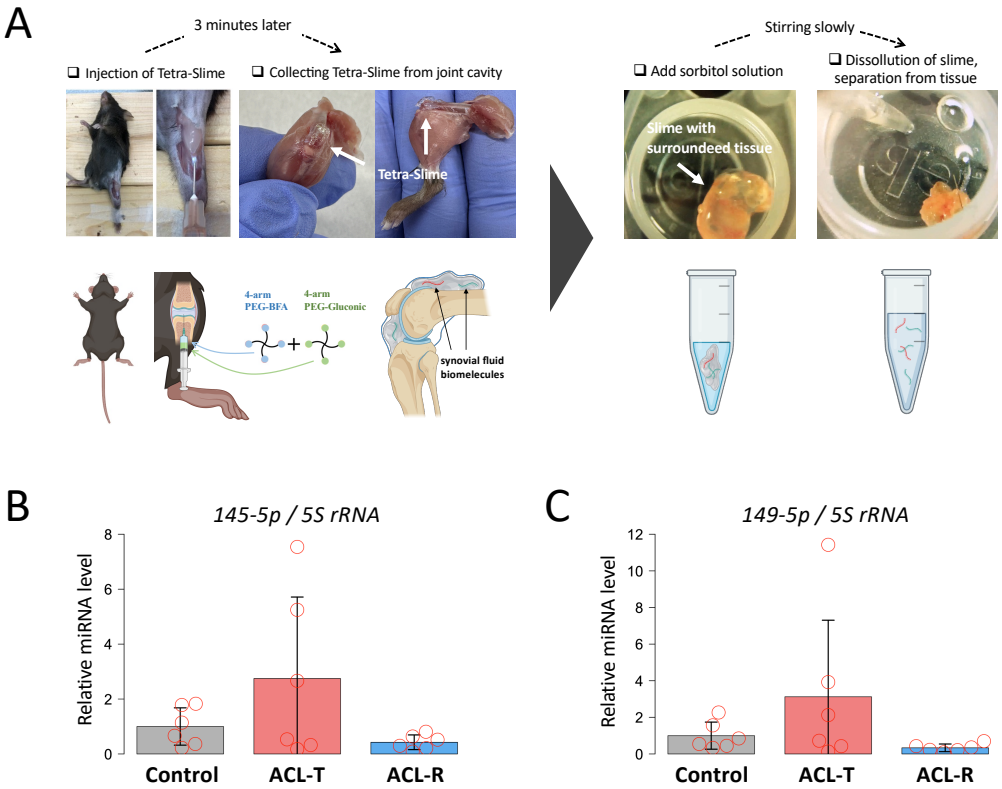

Fig. 7. (A) Conceptual diagram of a novel method to collect synovial fluid biomolecules in the murine knee joints using Tetra-Slime. After dissolving 4-arm PEG-BFA and 4-arm PEG-Gluconic in 50 mM phosphate-buffered saline (pH 3.0) and adjusting the concentration to 0.2 g/ml, 50 µl was injected into the knee joint. 3 minutes later, solidified Tetra-Slime including synovial fluid was collected and it was resolved by 100 µL of sorbitol solution with a 0.5 g/ml concentration to separate from the surrounding intra-articular tissue. (B-C) The ACL-T group exhibited an increase of miR145-5p and miR149-5p expression in synovial fluid compared to the Control and ACL-R groups at 2 weeks. Data are presented as the mean ± 95% CI.

399

400 # Discussion

401 Synovial fluid analysis contributes to understanding molecular changes within knee
402 joint capsule and detecting OA earlier. However, analysis methods for mice had not been
403 established. In this study, we developed a novel method to collect and analyze synovial fluid
404 miRNAs in murine knee joints using Tetra-slime, which can adjust its hardness. Using this
405 method, we aimed to investigate knee OA pathology in each Invasive and Non-Invasive ACL
406 injury mouse models in terms of tissue-interaction via synovial fluid. Our data clarified that
407 acute synovitis in the ACL-T model induced secondary cartilage degeneration in the early
408 stage compared with the ACL-R model; however, the progression of these histological
409 changes was identical between both models in the late stage. Real-time PCR revealed that
410 *Mmp-3*, *Tnf-α*, and M1 macrophage activation in synovium might be involved in the
411 secondary cartilage degeneration. We successfully established a novel method for analyzing
412 murine synovial fluid, and dPCR revealed that circulating *miR145-5p* and *miR149-5p* in
413 synovial fluid may suppress OA progression caused by acute synovitis.

414 Mechanical stress plays a significant role in maintaining intra-articular homeostasis;
415 however, excessive stress induces synovitis and cartilage degeneration. During the early stage
416 of OA progression, synovitis is generally initiated and driven by damage-associated
417 molecular patterns (DAMPs) released from the extracellular matrix to the synovial fluid.[34-37]

418 DAMPs activate TLRs in the synovium, leading to cartilage degeneration through the
419 inflammatory mediators and MMPs.[38, 39] In this study, we demonstrated that the ACL-T
420 group significantly induced synovitis at 2 weeks compared with the ACL-R group. However,
421 there was no difference in joint instability between groups. Furthermore, real-time PCR
422 revealed no differences in *Tlr4* expression, the receptor for DAMPs [39] in the synovium,
423 among all groups. Considering that synovitis is generally induced by DAMPs through
424 cartilage degeneration, our result indicates that acute synovitis at 2 weeks in the ACL-T group
425 is attributed to the surgical intervention, not secondary pathogenesis. Previous studies
426 reported that cartilage degeneration following ACL injury initiates in the medial compartment
427 due to joint instability. [40-42] However, the OARSI score in the lateral compartment of the
428 ACL-T group was significantly higher than that of the ACL-R group at 2 weeks, suggesting
429 that acute synovitis might cause secondary cartilage degeneration in the early stage.
430 We revealed the effect of acute synovitis on cartilage degeneration during the OA
431 progression, then performed molecular biological analysis to examine the tissue interaction
432 between synovium and cartilage. MMP-3 in the synovium of OA patients was positively
433 related to the severity [43], and it degrades cartilage ECM and activates other serine proteases
434 besides MMP-1, MMP-9, and MMP-13 [44]. Previous studies have shown that the depletion of
435 synovial macrophages suppresses MMP-3 expression both in vivo [45]and in vitro[46]. Our data
436 showed that *Mmp-3*, *Tnf-α*, *Ifn-γ*, and *inos* were upregulated in the synovium of the ACL-T

437 group at 2 weeks, which supported a previous study. This suggests that M1 macrophages
438 likely affected the tissue interaction between acute synovitis and secondary cartilage
439 degeneration. Unlike the synovial molecular changes, the expression of *Mmp-3* and *Tnf-α* in
440 the cartilage increased significantly in the ACL-R group compared with the ACL-T group at
441 the same time point. These results suggest that articular cartilage may initiate intra-articular
442 degeneration more preferentially than synovium in the OA induced by joint instability and
443 less inflammation, which supports our previous study. [21] The expression of *Timp-1*, which is
444 an MMP-3 inhibitor [26], was also elevated significantly; therefore, it is estimated that cartilage
445 degeneration occurred slightly in the ACL-R model at 2 weeks.

446 Synovial fluid is the most suitable biofluid for exploring the onset mechanism of OA
447 because it directly reflects the changes in various intra-articular tissues. The importance of
448 miRNA epigenetic regulation as a cellular communication is becoming increasingly
449 recognized, and many studies have recently demonstrated its effectiveness in the synovial
450 fluid of OA patients [47, 48]. However, no study investigated the changes in synovial fluid
451 miRNA in the mice OA model due to the difficulty of collection and analysis. Here, we
452 established a novel method to collect synovial fluid effectively from the murine knee joint
453 using Tetra-Slime. dPCR showed a non-specific reaction of Tetra-Slime to 5s rRNA
454 expression (Supplementary result), meaning that it enabled the analysis of synovial fluid
455 components accurately. Previous studies reported that TNF-α downregulated both miR145-5p

456 [31] and miR149-5p [32] in chondrocytes, leading to cartilage degeneration. However, our results
457 clarified that circulating *miR145-5p* and *miR149-5p* expression in synovial fluid increased
458 moderately at 2 weeks in the ACL-T group despite inducing moderate OA pathology. This
459 suggests that miR145-5p and miR149-5p in synovial fluid might be produced from
460 chondrocytes to protect against secondary cartilage degeneration by acute synovitis.

461 In contrast to the histological OA pathologies observed at 2 weeks, there were no
462 significant differences in the synovitis and OARSI score at 6 and 10 weeks between the ACL-
463 T and ACL-R groups. This suggests that mechanical stress with joint instability has a much
464 greater impact on cartilage degeneration in the long term, rather than acute synovitis, in the
465 progression of OA.

466 This study has two limitations: first, we could not exclude the intra-patellar fat pad
467 (IFP) when synovium was collected from the knee joint. Therefore, the result of real-time
468 PCR for synovium might reflect the biological changes of IFP to synovitis and mechanical
469 stress. The second is that miRNA-derived cells were not clarified. Synovial fluid components
470 reflect biological changes of various articular tissues, not only synovium and cartilage;
471 therefore, we need to perform additional in vitro experiments to investigate the tissue
472 interaction between synovium and cartilage in detail.

473 In conclusion, we successfully established a novel method for collecting synovial
474 fluid in the murine knee joint using Tetra-slime. During the OA progression, acute synovitis

475 led to secondary cartilage degeneration in the early stage, which might be attributed to the

476 increase of MMP-3, TNF-α, and M1 macrophage activation in the synovium. Among this

477 tissue interaction, synovial fluid might play a role in preventing cartilage degeneration by

478 increasing miR145-5p and miR149-5p. Whereas in the middle and late stages, mechanical

479 stress was a more critical factor in the progression of cartilage degeneration rather than

480 synovitis (Fig. 8).

481

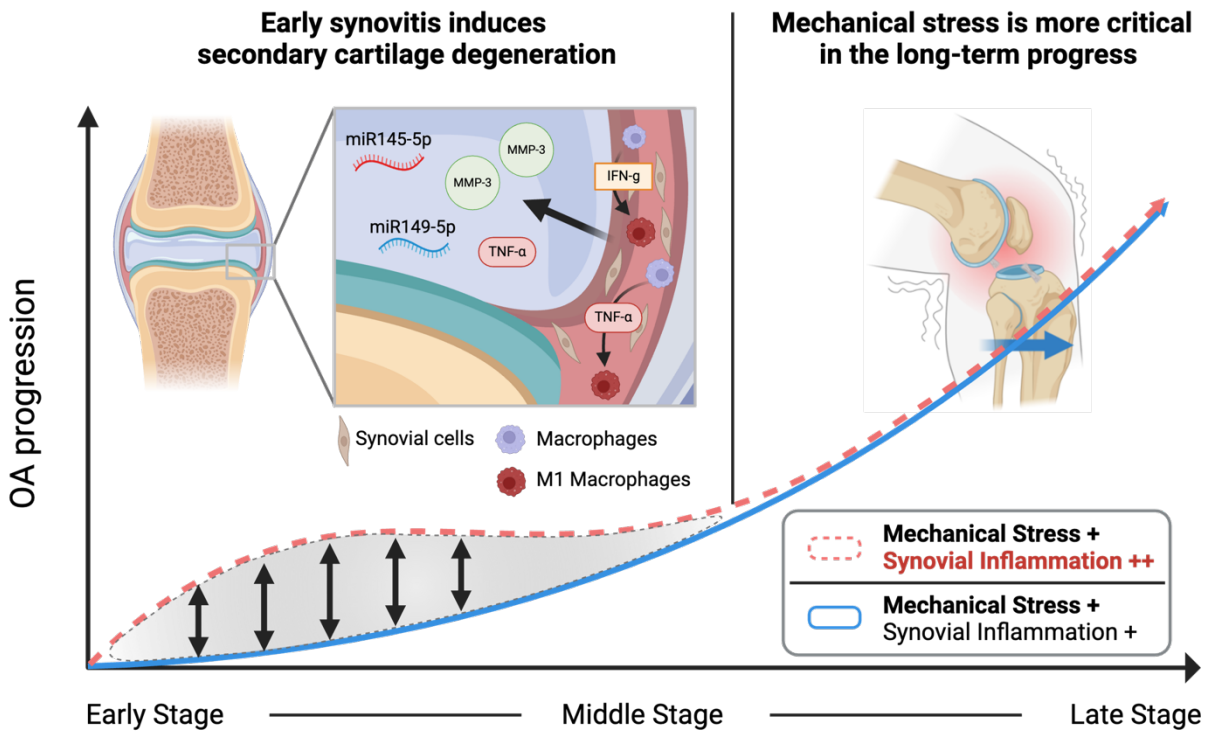

482

483 Fig. 8. Schematic mechanism of OA development with acute synovitis and chronic
484 mechanical stress. Acute synovitis caused secondary cartilage degeneration in the early stage
485 and MMP-3, TNF-α, and M1 macrophage activation in the synovium were involved in this
486 tissue interaction. Furthermore, miR145-5p and miR149-5p were secreted into the synovial
487 fluid to protect secondary cartilage deterioration during the same time. Unlike the early stage,
488 continuous mechanical stress had a much greater impact on cartilage degeneration rather than
489 synovitis after the middle stage.

490

Acknowledgments

The author(s) received no financial support for the research, authorship, and/or publication of this article. The study design and summary scheme were created with BioRender.com.

Author contributions

All authors approved the final submitted manuscript.

Study design: KT.

Data collection: KT

Histological analysis: KT, KA, and SE.

Biological analysis: KT, SY, TS, and TK.

Manuscript composition: KT, TK.

Role of funding source

This study was supported by the Grant-in-Aid for JSPS Research Fellows (22J23384) to KT and Grant-in-Aid for JSPS Challenging Research (Exploratory)(21K19724) to TK.

Competing interest statement

All authors have no conflicts of interest related to the manuscript.

References

1. Han S. Osteoarthritis year in review 2022: biology. Osteoarthritis Cartilage 2022;30:1575–82.
2. Karsdal MA, Christiansen C, Ladel C, Henriksen K, Kraus VB, Bay–Jensen AC. Osteoarthritis—a case for personalized health care? Osteoarthritis Cartilage 2014;22:7–16.
3. Kuyinu EL, Narayanan G, Nair LS, Laurencin CT. Animal models of osteoarthritis: classification, update, and measurement of outcomes. J Orthop Surg Res 2016;11:19.
4. Peters H, Rockel JS, Little CB, Kapoor M. Synovial fluid as a complex molecular pool contributing to knee osteoarthritis. Nat Rev Rheumatol 2025;21:447–64.
5. Plsikova Matejova J, Spakova T, Harvanova D, Lacko M, Filip V, Sepitka R, *et al.* A Preliminary Study of Combined Detection of COMP, TIMP–1, and MMP–3 in Synovial Fluid: Potential Indicators of Osteoarthritis Progression. Cartilage 2021;13:1421S–30S.
6. Rajandran SN, Ma CA, Tan JR, Liu J, Wong SBS, Leung YY. Exploring the Association of Innate Immunity Biomarkers With MRI Features in Both Early and Late Stages Osteoarthritis. Front Med (Lausanne) 2020;7:554669.
7. Tavallaee G, Rockel JS, Lively S, Kapoor M. MicroRNAs in Synovial Pathology Associated With Osteoarthritis. Front Med (Lausanne) 2020;7:376.
8. Cortez MA, Bueso–Ramos C, Ferdin J, Lopez–Berestein G, Sood AK, Calin GA. MicroRNAs in body fluids—the mix of hormones and biomarkers. Nat Rev Clin Oncol 2011;8:467–77.
9. Li YH, Tavallaee G, Tokar T, Nakamura A, Sundararajan K, Weston A, *et al.* Identification of synovial fluid microRNA signature in knee osteoarthritis: differentiating early– and late–stage knee osteoarthritis. Osteoarthritis Cartilage 2016;24:1577–86.
10. Xie W, Su W, Xia H, Wang Z, Su C, Su B. Synovial Fluid MicroRNA–210 as a Potential Biomarker for Early Prediction of Osteoarthritis. Biomed Res Int 2019;2019:7165406.
11. Boffa A, Merli G, Andriolo L, Lattermann C, Salzmann GM, Filardo G. Synovial Fluid Biomarkers in Knee Osteoarthritis: A Systematic Review and Quantitative Evaluation Using BIPEDs Criteria. Cartilage 2021;13:82S–103S.
12. Sousa–Valente J, Calvo L, Vacca V, Simeoli R, Arevalo JC, Malcangio M. Role of TrkA signalling and mast cells in the initiation of osteoarthritis pain in the monoiodoacetate model. Osteoarthritis Cartilage 2018;26:84–94.
13. Keeble J, Blades M, Pitzalis C, Castro da Rocha FA, Brain SD. The role of substance P in microvascular responses in murine joint inflammation. Br J Pharmacol 2005;144:1059–66.
14. Keeble J, Russell F, Curtis B, Starr A, Pinter E, Brain SD. Involvement of transient receptor potential vanilloid 1 in the vascular and hyperalgesic components of joint inflammation. Arthritis Rheum 2005;52:3248–56.

15. Seifer DR, Furman BD, Guilak F, Olson SA, Brooks SC, 3rd, Kraus VB. Novel synovial fluid recovery method allows for quantification of a marker of arthritis in mice. Osteoarthritis Cartilage 2008;16:1532–8.
16. Hong S, Yu T, Wang Z, Lee CH. Biomaterials for reliable wearable health monitoring: Applications in skin and eye integration. Biomaterials 2025;314:122862.
17. Wang H. Biomaterials in Medical Applications. Polymers (Basel) 2023;15.
18. Trucillo P. Biomaterials for Drug Delivery and Human Applications. Materials (Basel) 2024;17.
19. Fang G, Bian Z, Liu D, Wu G, Wang H, Wu Z, *et al.* Water–soluble diboronic acid–based fluorescent sensors recognizing d–sorbitol. New Journal of Chemistry 2019;43:13802–9.
20. Katashima T, Kudo R, Naito M, Nagatoishi S, Miyata K, Chung UI, *et al.* Experimental Comparison of Bond Lifetime and Viscoelastic Relaxation in Transient Networks with Well–Controlled Structures. ACS Macro Lett 2022;11:753–9.
21. Takahata K, Arakawa K, Enomoto S, Usami Y, Nogi K, Saitou R, *et al.* Joint instability causes catabolic enzyme production in chondrocytes prior to synovial cells in novel non–invasive ACL ruptured mouse model. Osteoarthritis Cartilage 2022.
22. Arakawa K, Takahata K, Enomoto S, Oka Y, Ozone K, Nakagaki S, *et al.* The difference in joint instability affects the onset of cartilage degeneration or subchondral bone changes. Osteoarthritis Cartilage 2022;30:451–60.
23. Glasson SS, Chambers MG, Van Den Berg WB, Little CB. The OARSI histopathology initiative – recommendations for histological assessments of osteoarthritis in the mouse. Osteoarthritis Cartilage 2010;18 Suppl 3:S17–23.
24. Krenn V, Morawietz L, Burmester GR, Kinne RW, Mueller–Ladner U, Muller B, *et al.* Synovitis score: discrimination between chronic low–grade and high–grade synovitis. Histopathology 2006;49:358–64.
25. Livak KJ, Schmittgen TD. Analysis of relative gene expression data using real–time quantitative PCR and the 2(–Delta Delta C(T)) Method. Methods 2001;25:402–8.
26. Takahashi K, Goomer RS, Harwood F, Kubo T, Hirasawa Y, Amiel D. The effects of hyaluronan on matrix metalloproteinase–3 (MMP–3), interleukin–1a(IL–1a), and tissue inhibitor of metalloproteinase–1 (TIMP–1) gene expression during the development of osteoarthritis. Osteoarthritis Cartilage 1999;2:182–90.
27. Zhang H, Cai D, Bai X. Macrophages regulate the progression of osteoarthritis. Osteoarthritis Cartilage 2020;28:555–61.
28. Wu CL, Harasymowicz NS, Klimak MA, Collins KH, Guilak F. The role of macrophages in osteoarthritis and cartilage repair. Osteoarthritis Cartilage 2020;28:544–54.
29. Fernandes TL, Gomoll AH, Lattermann C, Hernandez AJ, Bueno DF, Amano MT. Macrophage: A Potential Target on Cartilage Regeneration. Front Immunol 2020;11:111.
30. Zhao K, Ruan J, Nie L, Ye X, Li J. Effects of synovial macrophages in osteoarthritis. Front Immunol 2023;14:1164137.

31. Hu G, Zhao X, Wang C, Geng Y, Zhao J, Xu J, *et al.* MicroRNA-145 attenuates TNF-alpha-driven cartilage matrix degradation in osteoarthritis via direct suppression of MKK4. Cell Death Dis 2017;8:e3140.
32. Santini P, Politi L, Vedova PD, Scandurra R, Scotto dAbusco A. The inflammatory circuitry of miR-149 as a pathological mechanism in osteoarthritis. Rheumatol Int 2014;34:711-6.
33. Chiu YS, Bamodu OA, Fong IH, Lee WH, Lin CC, Lu CH, *et al.* The JAK inhibitor Tofacitinib inhibits structural damage in osteoarthritis by modulating JAK1/TNF-alpha/IL-6 signaling through Mir-149-5p. Bone 2021;151:116024.
34. de Lange-Brokaar BJ, Ioan-Facsinay A, van Osch GJ, Zuurmond AM, Schoones J, Toes RE, *et al.* Synovial inflammation, immune cells and their cytokines in osteoarthritis: a review. Osteoarthritis Cartilage 2012;20:1484-99.
35. Nefla M, Holzinger D, Berenbaum F, Jacques C. The danger from within: alarmins in arthritis. Nat Rev Rheumatol 2016;12:669-83.
36. Lopes EBP, Filiberti A, Husain SA, Humphrey MB. Immune Contributions to Osteoarthritis. Curr Osteoporos Rep 2017;15:593-600.
37. Lambert C, Zappia J, Sanchez C, Florin A, Dubuc JE, Henrotin Y. The Damage-Associated Molecular Patterns (DAMPs) as Potential Targets to Treat Osteoarthritis: Perspectives From a Review of the Literature. Front Med (Lausanne) 2020;7:607186.
38. Liu-Bryan R. Synovium and the innate inflammatory network in osteoarthritis progression. Curr Rheumatol Rep 2013;15:323.
39. Bartels YL, van Lent P, van der Kraan PM, Blom AB, Bonger KM, van den Bosch MHJ. Inhibition of TLR4 signalling to dampen joint inflammation in osteoarthritis. Rheumatology (Oxford) 2024;63:608-18.
40. Pauly HM, Larson BE, Coatney GA, Button KD, DeCamp CE, Fajardo RS, *et al.* Assessment of cortical and trabecular bone changes in two models of post-traumatic osteoarthritis. J Orthop Res 2015;33:1835-45.
41. Maerz T, Newton MD, Kurdziel MD, Altman P, Anderson K, Matthew HW, *et al.* Articular cartilage degeneration following anterior cruciate ligament injury: a comparison of surgical transection and noninvasive rupture as preclinical models of post-traumatic osteoarthritis. Osteoarthritis Cartilage 2016;24:1918-27.
42. Gilbert SJ, Bonnet CS, Stadnik P, Duance VC, Mason DJ, Blain EJ. Inflammatory and degenerative phases resulting from anterior cruciate rupture in a non-invasive murine model of post-traumatic osteoarthritis. J Orthop Res 2018;36:2118-27.
43. Chen JJ, Huang JF, Du WX, Tong PJ. Expression and significance of MMP3 in synovium of knee joint at different stage in osteoarthritis patients. Asian Pac J Trop Med 2014;7:297-300.
44. Murphy G, Nagase H. Progress in matrix metalloproteinase research. Mol Aspects Med 2008;29:290-308.

621 45. Blom AB, van Lent PL, Libregts S, Holthuysen AE, van der Kraan PM, van Rooijen N, *et al*. Crucial
622 role of macrophages in matrix metalloproteinase–mediated cartilage destruction during
623 experimental osteoarthritis: involvement of matrix metalloproteinase 3. Arthritis Rheum
624 2007;56:147–57.
625 46. Bondeson J, Wainwright SD, Lauder S, Amos N, Hughes CE. The role of synovial macrophages and
626 macrophage–produced cytokines in driving aggrecanases, matrix metalloproteinases, and other
627 destructive and inflammatory responses in osteoarthritis. Arthritis Res Ther 2006;8:R187.
628 47. Munjal A, Bapat S, Hubbard D, Hunter M, Kolhe R, Fulzele S. Advances in Molecular biomarker for
629 early diagnosis of Osteoarthritis. Biomol Concepts 2019;10:111–9.
630 48. Palma AD, Cheleschi S, Pascarelli NA, Tenti S, Galeazzim M, Fioravanti A. Do microRNAs have a key
631 epigenetic role in osteoarthritis and in mechanotransduction? Clin Exp Rheumatol 2016;35 518–
632 26.
633